Generation of a Medaka Fish Model of Propionic Acidemia for Development of Novel Therapies.

Thesis

VIRGINIA MARIA GINOCCHIO, M.D.

Generation of a medaka fish model of propionic acidemia for development of novel therapies.

Ph.D. Thesis

The Open University

Affiliated Research Centre: **Telethon institute of Genetics and Medicine (TIGEM)**

Director of Studies: Prof. **Nicola Brunetti-Pierri**

Thesis submitted in accordance with the requirements of The Open University for the degree “Doctor of Philosophy”

September 2016

Table of Contents

Abstract

Propionic acidemia (PA) is an autosomal recessive inborn error of metabolism caused by deficiency of the mitochondrial enzyme propionyl-CoA carboxylase (PCC). The disease presents with acute, recurrent and life-threatening crises of metabolic decompensation starting from the newborn period. Patients also suffer from multi-organ complications, neurological dysfunction, and cardiomyopathy. Despite available treatments, disease mortality and morbidity remain elevated and investigation of novel and more effective therapies is highly needed.

I have generated a PA model in medaka fishes (*Oryzias latipes)* using TALENs targeting the *pccb* medaka gene, encoding one of the subunits of PCC. The *pccb*$^{del/del}$ medaka recapitulates the clinical and biochemical phenotype of human patients. Affected medaka larvae showed early lethality and severe neurological impairment as shown by reduced and abnormal movements. Livers and hearts of *pccb*$^{del/del}$ larvae exhibited increased lipid droplets, likely as a consequence of impaired mitochondrial β-oxidation. Importantly, *pccb*$^{del/del}$ larvae showed a significant increase in the levels of propionylcarnitine (C3), the biochemical hallmark of the disease. Administration of a low-protein diet improved the survival of *pccb*$^{del/del}$ larvae. Because PCC deficiency induces depletion of Krebs cycle intermediates, I investigated the efficacy of an anaplerotic therapy in *pccb*$^{del/del}$ medaka fishes. The anaplerotic therapy comprising sodium citrate, ornithine α-ketoglutarate, and glutamine resulted in significant improvements of both survival and locomotor activity in *pccb*$^{del/del}$ larvae.

Given its small size, easy handling and large number of progeny, the PA medaka model is suitable for rapid investigation of novel drugs by large-scale drug screening. I have set a drug screening assay on whole fishes using the clinically relevant locomotor

activity as read-out of the assay. This large drug screening has the potential to lead to the identification of small molecule drugs already approved for use in humans that have the potential to be rapidly translated in clinical applications.

List of abbreviations

AAV, adeno-associated virus

BC, biotin carboxylase

BCCP, biotin carboxyl carrier protein domains

CNS, central nervous system

CoA, coenzyme A

CPSI, carbamoyl phosphate synthetase I

CT, carboxyltransferase

Dpf, days post fertilization

FDA, Food and Drug Administration

GFP, green fluorescent protein

H&E, hematoxylin-eosin

HRP, horseradish peroxidase

IHC, immunohistochemistry

MMA, methylmalonic acidemia

OKG, ornithine-α-ketoglutarate

PA, propionic acidemia

PBS, phosphate buffered saline

PCC, propionyl-CoA carboxylase

RFP, red fluorescent protein

SD, standard deviation

SE, standard error

TALEN, transcription activator-like effector nucleases

wt, wild-type

Introduction

Propionic acidemia

Propionic acidemia (PA) (OMIM 606054) is an autosomal recessive inborn error of metabolism, first described in 1961 as "ketotic hyperglycinemia" for the coexistence of ketoacidosis and increased levels of glycine in blood and urine [1]. In 1968 a disorder characterized by metabolic acidosis and high levels of propionic acid in blood was described and indicated for the first time as "propionic acidemia" [2]. Few years later, the biochemical basis of the disease was clarified and the identity between "ketotic hyperglycinemia" and "propionic acidemia" was established [3, 4].

The disorder has an incidence of about 1:50,000 to 1:100,000; although the disease incidence is variable among different populations, it is higher in Inuit in Greenland and in Saudi Arabia, while Japanese people show higher incidence of a mild form of the disease [5-9].

PA is caused by deficiency of the biotin-dependent propionyl-CoA carboxylase (PCC) (E.C. 6.4.1.3), the mitochondrial enzyme that converts propionyl-CoA into D-methylmalonyl-CoA. Methylmalonyl-CoA is then converted into succinyl-CoA, a Krebs cycle intermediate (**Figure 1**). Propionyl-CoA is the product of the catabolism of different metabolites: valine, isoleucine, methionine, threonine (accounting for about 50% of total propionic acid), odd-chain fatty acids (accounting for about 25%), while degradation of cholesterol side-chain seems to be of little quantitative significance [10, 11]. Propionate is also formed by gut bacteria, accounting for about 25% of total production [11].

PCC is a heterododecamer composed of six α-subunits encoded by the *PCCA* gene and six β-subunits encoded by the *PCCB* gene [10]. The crystal structure of PCC has

been characterized from bacteria *Ruegeria pomeroyi* and *Roseobacter denitrificans* [12]. PCC is a heterododecamer with a molecular weight of 750 kDa, composed of six β-subunits forming a central cylindric core and six α-subunits arranged as monomers decorating the central hexamer, each of them interacting with a single β-subunit. The α-subunits interact with the cofactor biotin and contain the biotin carboxylase (BC) and the biotin carboxyl carrier protein domains (BCCP), while the β-subunit is responsible for carboxyltransferase (CT) activity. The α-subunit also contains a domain responsible for interaction between the BC domain and the CT domain of β-subunit that has been called BT domain [12]. The β-subunits work as dimers and the active site is located at the interface of the two β monomers. Disease-causing mutations usually impair substrate binding or catalytic activity or hamper the assembly of the holoenzyme.

Mutations affecting either *PCCA* or *PCCB* gene can cause the disease and approximately 60% of cases of PA patients of Caucasian origin harbour mutations in the *PCCB* gene [13-15]. At least 80 different mutations have been described so far both in *PCCA* and *PCCB*, including missense, nonsense, splicing mutations, small insertions and deletions, and large deletion (the latter only for the *PCCA* gene) [15-17].

The spectrum of clinical presentations of PA ranges from severe neonatal-onset to mild late-onset disease. The age of onset seems to be related to residual enzyme activity and severity of the disease [18]. The most common classic form of PA typically presents in the newborn period with acute onset of metabolic decompensation. During pregnancy, toxic metabolites are cleared by the maternal placenta, and thus affected patients appear healthy at birth, but develop in the first hours or days of life nonspecific symptoms including vomiting, refusal to feed, hypotonia, and lethargy. Clinical manifestations are due to severe metabolic alterations including acidosis, ketosis, and hyperammonemia. If untreated, the disease precipitates in encephalopathy, cardio-respiratory failure, and death [19]. In patients with later onset, the disease usually

presents in the first years of life, more often with an acute metabolic crisis, while less common is the diagnosis in patients only manifesting chronic or intermittent symptoms [18].

If they survive the first episode of metabolic decompensation, patients with both early- and late-onset forms have a life-long risk of recurrent, potentially lethal, acute decompensations that are usually precipitated by fasting, intercurrent illnesses, infections, surgery, or other stressful conditions that induce catabolic stress [19]. Moreover, in both forms patients can also manifest chronic symptoms and develop multi-organ complications. Many affected children present failure to thrive and growth retardation; microcephaly has also been observed in about 30% of cases [20, 21]. Even if correctly managed, almost all patients have some degree of central nervous system (CNS) involvement. Neurological symptoms include hypotonia, seizures, developmental delay, cognitive impairment, movement disorders (ataxia, chorea), dystonia, and spasticity. Patients can also manifest acute encephalopathy and stroke-like episodes called “metabolic strokes” that frequently involve basal ganglia and result in movement disorders [20-22]. Relatively common neuroimaging findings accompanying neurological degeneration are brain atrophy, white matter and basal ganglia abnormalities [21, 22]. Cardiomyopathy is observed in about one third of cases and is a life-threatening complication. Although hypertrophic cardiomyopathy is also described, patients more often present with dilated cardiomyopathy. The heart involvement may also be isolated and may not be related to the severity or the time of onset of the disease. ECG abnormalities, including prolonged QT interval, can also be present and increase the risk of sudden death [23-25]. Hematological and immunological abnormalities including neutropenia, thrombocytopenia, and rarely pancytopenia can be observed in PA patients but their frequency has not been estimated [26]. Recurrent pancreatitis represent another rare but potentially severe complication of PA [26].

Pathogenesis of PA

Even if the molecular defect underlying the disease has been known for many years, the pathogenesis of multiple biochemical and clinical abnormalities observed in PA is still the object of investigations.

Several metabolites that are undetected or detected at low levels in normal subjects are increased in blood and urine of patients with PA. 3-OH propionate, methylcitrate, propionylcarnitine, propionylglycine, and tiglylglycine are the biochemical hallmarks of PA [10]. They result from accumulation of propionyl-CoA and its by-products as a consequence of the enzyme block and activation of alternative pathways, such as conjugation of propionate and other metabolites with carnitine and glycine [1, 27].

Large amounts of ketones are formed as by-products of metabolites accumulating upstream of the enzyme defect, leading to severe and sometimes untreatable metabolic acidosis [10]. The hyperglycinemia is due to impaired glycine cleavage caused by direct inhibition by propionyl-CoA and other CoA esters of the glycine cleavage enzyme [28]. Glycine acts in the CNS as a neurotransmitter and its increased levels may contribute to the neurological manifestations.

Hyperammonemia has been related for a long time to competitive inhibition of N-acetylglutamate synthase by propionyl-CoA and production of N-propionylglutamate instead of N-acetylglutamate with consequent reduction of N-acetylglutamate levels and secondary inhibition of carbamoylphosphate synthetase I (CPS I) (**Figure 1**) [29]. However, several evidences suggest that another mechanism may be responsible for the hyperammonemia. Reduced levels of glutamate and glutamine [30] result in reduced formation of N-acetylglutamate that leads to impairment of the urea cycle and depletion of glutamine that can further contribute to the defect of ammonia handling (**Figure 1**).

The Krebs cycle is impaired in PA patients because of a number of mechanisms including; i) reduced production of succinyl-CoA; ii) propionyl-CoA competes with

acetyl-CoA and combines with oxaloacetate in the reaction catalyzed by citrate synthase to form methylcitrate instead of citrate, leading to further depletion of essential metabolites (oxaloacetate and citrate); iii) methylcitrate is a potent inhibitor of the Krebs cycle enzymes citrate synthase, aconitase, and isocitrate dehydrogenase; iv) propionyl-CoA and other short-chain acyl-CoA inhibit pyruvate dehydrogenase and α-ketoglutarate dehydrogenase [31, 32]. In summary, the defect of the Krebs cycle is both the consequence of depletion of essential metabolites and enzyme inhibition by toxic metabolites (**Figure 1**).

It has been hypothesized that in PA patients the Krebs cycle could be replenished by increased production of α-ketoglutarate deriving from increased deamination of glutamine and glutamate that results from a shift in the equilibrium of the reactions catalyzed by glutamate dehydrogenase and glutaminase. This leads to depletion of the glutamine/glutamate pool and increased ammonia formation (**Figure 1**) [33].

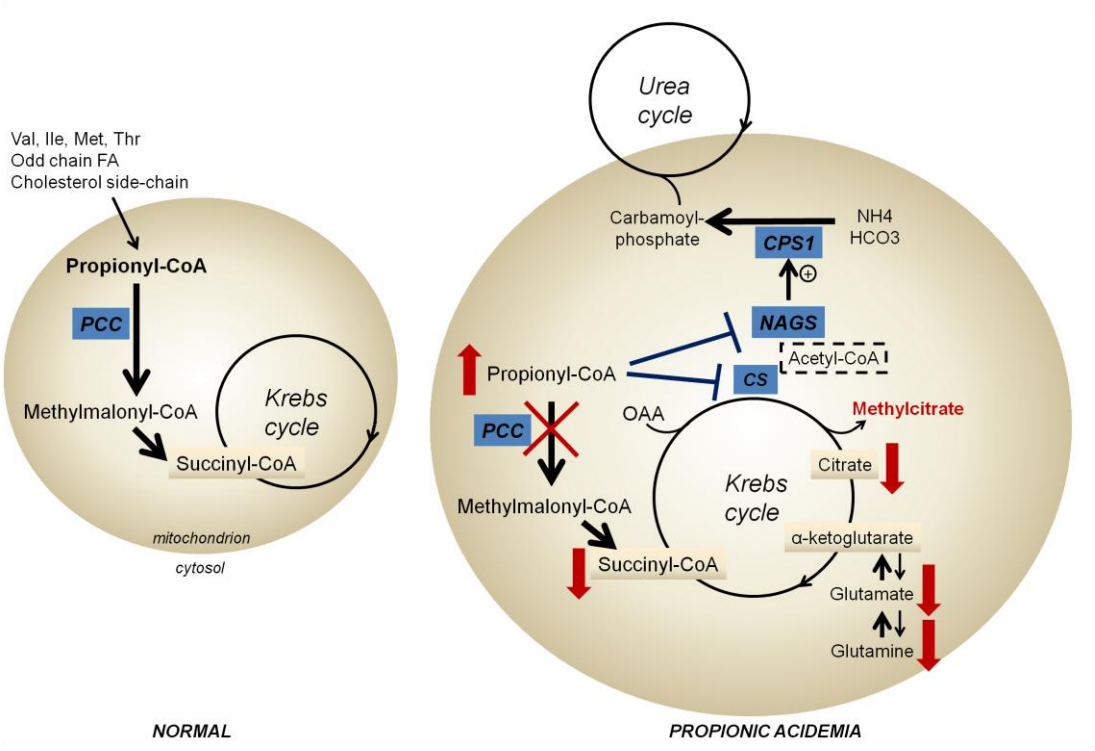

Figure 1. Schematic representation of the main metabolic pathways involved in PA. Propionyl-CoA is the product of the catabolism of some amino acids, odd chain fatty acids and cholesterol side-chain. The

PCC defect causes reduced supply of succinyl-CoA to the Krebs cycle and accumulation of propionyl-CoA that in turn interferes with several enzyme reactions. In particular, competition with acetyl-CoA in the reactions catalyzed by citrate synthase (CS) and N-acetylglutamate synthase (NAGS) leads to reduced production of citrate (replaced by the toxic metabolite methylcitrate) and reduced supply of carbamoylphosphate to the urea cycle, respectively. Increased conversion of glutamate into α-ketoglutarate (to replenish the Krebs cycle) could explain the reduced level of glutamate and glutamine that are observed in PA patiens. OAA, oxaloacetate; CS, citrate synthase; NAGS, N-acetylglutamate synthase; CPS1, carbamoylphosphate synthetase 1; PCC, propionyl-CoA carboxylase.

Moreover, multiple evidences suggest a defect in mitochondrial energy metabolism in PA patients. Krebs cycle impairment leads to reduced production of ATP and reduced supply of NADH and FADH2 to the mitochondrial electron transport chain. In addition, secondary inhibition of several complexes of mitochondrial electron transport chain has been observed both *in vivo* and *in vitro* [25, 32, 34-38]. Impaired energy metabolism can explain multi-organ toxicity, particularly in tissues that are highly dependent on oxidative phosphorylation for energy production like brain, heart, and skeletal muscle. The occurrence of neurological and cardiac diseases even in the absence of metabolic decompensation suggests the involvement of local production of toxic metabolites or defect in energy production [25, 34, 39, 40]. In addition, reduced permeability of the blood brain barrier to dycarboxylic acids, with "trapping" of toxic metabolites in the CNS has been proposed to explain the neurologic damage [41, 42].

Treatment strategies for PA: state of the art

Without proper diagnosis and interventions, the prognosis of early onset disease is very poor with a mortality close to 100% [43]. In the last few years, there have been significant improvements in early diagnosis by expanded newborn screening based on C3-propionylcarnitine measurement by tandem mass spectrometry. However, treatment

of PA is challenging and even if current treatments have significantly improved long-term survival, the mortality of the disease remains still high and neurological sequelae are common [44].

Current therapies aim at reducing the production of propionyl-CoA from protein catabolism (low protein/high energy diet, avoidance of fasting and stressful events), reducing production of propionate by gut bacteria through antimicrobial drugs, and increasing propionyl-CoA excretion by carnitine administration [45, 46]. Carnitine supplementation is also given to compensate for secondary carnitine deficiency and preserve the free acyl-CoA pool. Treatment with the PCC enzyme cofactor biotin has been proposed although its efficacy has not been demonstrated [46]. Since hyperammonemia is related to inhibition of CPS I, administration of N-carbamylglutamate, a CPS I activator, is also used for treatment of hyperammonemia in PA. Administration of N-carbamylglutamate in PA patients has resulted in increased urea production and reduction of ammonia levels [47]. Nevertheless, even a careful dietetic and therapeutic management is not able to prevent life-threatening metabolic crisis and multi-organ complications.

Orthotopic liver transplantation is considered particularly in PA patients with frequent metabolic decompensations and poor response to dietary and pharmacological treatments [46]. Reduction of the frequency and intensity of the metabolic crises as well as positive effects on neurological and cardiac complications have been observed in patients who received liver transplantation [48, 49]. However, it is still unclear whether liver transplantation might prevent the metabolic strokes because of reports of metabolic strokes in transplanted patients [49]. Although the liver transplant restores enzyme function in liver, PCC remains deficient in the other tissues were it is expressed. Although current elective transplant procedures have significantly improved, liver transplantation remains an invasive procedure, with its own mortality and morbidity

related to rejection and other possible complications and to the need for life-long immunosuppression.

Gene therapy is a promising therapeutic approach for many inborn errors of metabolism including PA but there are also several obstacles preventing its application in the clinics. PA has often an acute onset in the first days of life, leading to the need for a rapid therapeutic intervention and the onset of gene expression by AAV-mediated gene transfer is not sufficiently rapid to correct the metabolic acidosis with acute onset in the newborn. In case of early administration, liver growth results in loss of episomal vector genomes and this will require vector re-administration that is hampered by the immune response against the viral vector. Indeed, loss of episomal AAV vector genomes as a consequence of liver growth has been observed in several studies [50, 51] and compromises long term correction of the phenotype. Moreover, early gene therapy administration in newborn mice has been associated to a potential risk of genotoxicity and hepatocarcinoma [52-54]. In particular, this finding has also been observed after early AAV gene therapy administration in the mouse model of methylmalonic acidemia (MMA), a disease biochemically and clinically related to PA due to the deficiency of the enzyme downstream of PCC [52]. Although the issue of insertional carcinogenesis in humans is still debated, the risk of cancer remains a concern particularly with vector administrations in the newborn period. Last but not least, PA is a multi-organ disease and it is unclear whether liver-directed gene therapy might result in resolution of all disease complications.

Animal models of PA

Two mouse models of PA have been generated thus far. The first is a *Pcca*-knockout mouse resulting in a severe phenotype and death in the first hours of life for

ketoacidosis. For the early lethality, this mouse is not suitable for investigation of the disease and experimental treatments [55]. To overcome these limitations, a transgenic mouse bearing a mutated human *PCCA* gene that encodes for an enzyme with reduced activity on the background of the *Pcca*-knockout mouse has been generated. This mouse survives into adulthood and thus, it is more suitable for therapeutic investigations [56], including the gene therapy [57, 58].

Open research questions and unmet medical needs

Available treatments for PA are unsatisfactory and despite therapy, patients still suffer from severe and invalidating complications and remain at risk of life-threatening metabolic crisis. Therefore, there is a high need for other therapies to be rapidly introduced in the clinics to improve the clinical outcomes of patients with PA. With this goal in mind, my thesis project has been focused on generating a fish model of PA for investigation of small molecule drugs for the treatment of the disease. Searching for drugs by high-throughput screening in animal models requires a large number of animals and is extremely expensive and unpractical in mice. Conversely, small fishes can be easily handled, are available in large number at low costs, and thus are suitable for high-throughput drug screening on whole animals. They have both the advantages of the small size and the substantial similarity with humans [59-61]. Over the past decades fish models have been largely used to investigate developmental processes and more recently, they have also shown to be effective in modelling inborn errors of metabolism, such as maple syrup urine disease, multiple acyl-CoA deficiency and Menkes disease [62-67].

As a fish model for PA, I have chosen the Japanese medaka fish (*Oryzias latipes*), a small teleost. Compared to zebrafish that have been more widely used, medaka fishes have the advantages of being easier to handle, they can develop at a wider range of

temperatures, and have a smaller, less redundant and well-draft genome of about 800 Mb [68]. They have been already used to model several human diseases and relevant human phenotypes have been recapitulated, demonstrating similarity in molecular pathways and physiological processes [69-73].

Aims of the project

My project had two main objectives:

- **Specific aim 1:** to generate and characterize a medaka fish model of PA.
- **Specific aim 2:** to investigate new therapeutic strategies for PA.

Methods

Animal strain and maintenance

Cab strain *Oryzias latipes* were kept in recirculating water aquaria at 28°C on a 12/12 h light/dark cycle. Embryos were collected by natural spawning and raised in Yamamoto solution at 26°C. All procedures on living animals were performed in anaesthesia by administration of tricaine mesylate (MS-222, Sigma Aldrich). Fishes were sacrificed by administration of a lethal dose of anaesthetic. All fish studies were conducted in accordance with the institutional guidelines for animal research.

Generation of PA medaka

I used custom-designed transcription activator-like effector nucleases (TALEN) to induce targeted mutagenesis in either *pcca* or *pccb* medaka genes. TALENs have been previously used successfully in medaka for targeted-mutagenesis in disease-causing genes [74, 75]. Genomic sequence of medaka *pcca* and *pccb* genes was retrieved from the Ensembl medaka genome browser (http://www.ensembl.org/Oryzias_latipes) and potential TALEN target sites in exon 4 of *pcca* gene and in exon 3 of *pccb* gene were identified using *TALEN Targeter* program at https://tale-nt.cac.cornell.edu/node/add/talen [76]. For *pcca*, the left (L) and right (R) recognition sequences and the spacer sequence were the following: L1 recognition sequence (16 bp): CGCTGTGAACCGCTATG; R1 recognition sequence (17 bp): GATCAAGACCTGTAAG; spacer sequence (17 bp): GTCTGGATGCCCATCCT (**Figure 2**). For *pccb* gene, the following recognition sequences were identified: L1 recognition sequence (18 bp): TCCCGGAGACAGCGTGGT; R1 recognition sequence (18 bp): AAACCAGCCTGCCGTTAA; spacer sequence (17 bp):

GACAGGCCGTGGCAGGA (**Figure 2**).

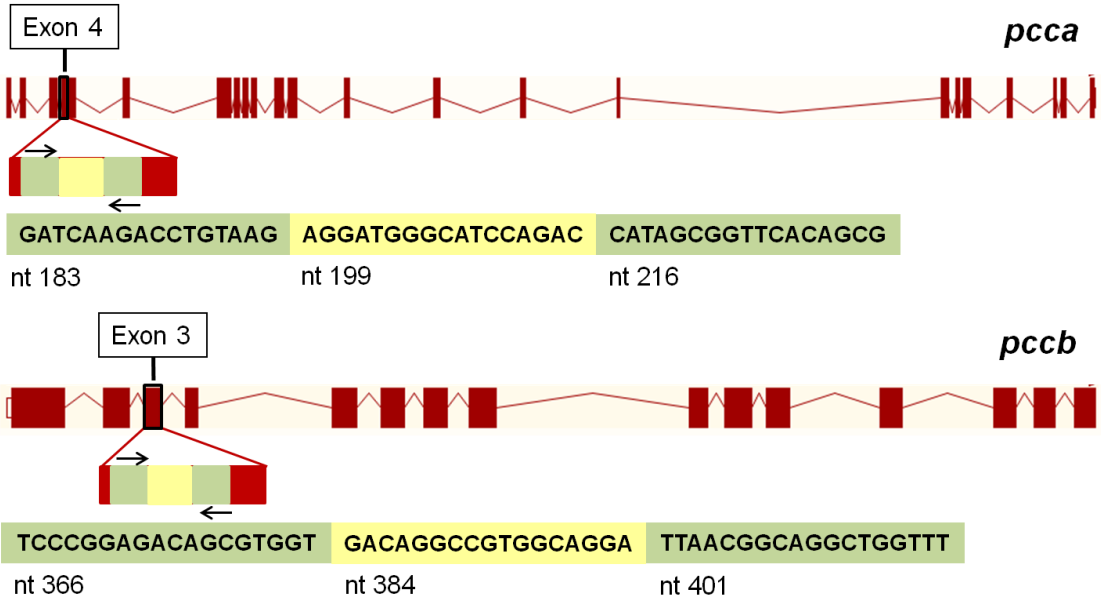

Figure 2. Genomic organization of *pcca* and *pccb* medaka genes and TALEN target sequences: recognition sequences are highlighted in green and spacer sequences are in yellow.

Custom-designed TALEN vectors were assembled by ZGenebio (ZGenebio Biotech Inc, Taiwan). For each target gene, two plasmids were produced, each one encoding a *Fok*I nuclease monomer and a TAL recognition domain able to recognize the left or right recognition sequence, respectively. The left (L) and right (R) plasmids (pZGB-3L and pZGB-3R) also included a SP6 promoter, an ampicillin-resistance gene, and a cDNA encoding the green or red fluorescent protein. Competent DH5α bacteria were transformed with the two plasmids and 500 ml of bacterial suspension, deriving from a single clone, was grown in medium containing ampicillin for plasmid preparation. Linearized *Not*I plasmids were extracted from agarose gel using a commercial kit (QIAquick Gel Extraction Kit, QIAGEN). RNA was synthesized *in vitro* using a commercial kit (mMESSAGE mMACHINE SP6 Transcription Kit, Ambion, Life Technologies).

A pair of TALEN RNA for each target gene was injected into fertilized eggs at about

1-2 cell-stage, at a concentration of 100 ng/µl by microinjection method [77]. Injected embryos were selected on the basis of GFP/RFP expression indicating successful translation of the injected RNA.

After hatching, a sample of more than 20 larvae were sacrificed and lysed for genomic DNA extraction. The target region on *pcca* and *pccb* gene was amplified by PCR and sequenced to determine the presence of TALEN-induced genomic changes in mosaic state. Primers for PCR amplification of the target sequences were the following: CACAGAGGTGAAGGAAAGTTG (for) and GCAGGTTCCACCTACTATTGAG (rev) for *pcca* gene; GAGCTCAGTTCTGTTCTGCAG (for) and GCACAGAAGATCTGTAAGGTGAG (rev), for *pccb* gene. G0-generation fishes (deriving from TALEN-injected embryos) and G1-generation fishes were genotyped using the genomic DNA extracted from the caudal fin. G0 mosaics were selected and mated with wild-type (wt) fishes to obtain heterozygous animals.

Phenotyping of PA medaka fishes

External features, heart rate and death were evaluated by direct observation with a stereomicroscope (Leica M205 FA). For most experimental procedures, affected larvae were selected by external phenotype and then cut into two halves. The caudal half was used for genomic DNA extraction and genotype confirmation by PCR and restriction digestion by *BsaJ*I enzyme (New England Biolabs Inc). Cranial halves, including the head and all internal organs, were used for experiments.

Survival was evaluated daily by direct observation. Death was established when absence of any reaction to repeated mechanical stimulation, as well as absence of heart beat for at least 10 s were observed. Total length and heart axis were measured on larval bright-field sagittal view, while head diameter was measured on dorsal view. Images

were acquired by stereomicroscope and analyzed by ImageJ software (www.imagej.net). Histologic examinations were performed on larvae fixed overnight in 4% paraformaldehyde/PTW (phosphate buffered saline (PBS)/Tween). For hematoxylin-eosin (H&E) staining, I used 4-µm sections obtained after dehydration with ethanol and paraffin embedding. For Oil Red staining, fixed larvae were dehydrated with cold sucrose and embedded in cryo embedding medium. 8-µm sections were cut and stained with Oil Red working solution, as previously described elsewhere [66].

Pccb protein studies

Pccb immunohistochemistry (IHC) was performed on 4-µm sections obtained from paraffin-embedded larvae using a rabbit polyclonal anti-pccb antibody (abcam ab96729) on at least 3 samples per group (*pccb*$^{del/del}$, wt). For western blot analysis, larval cranial halves were pooled and lysed in RIPA buffer (50 mM pH 7.4 Tris, 150 mM NaCl, 1% Triton, 1 mM EDTA, 0.1% SDS) with protease inhibitor cocktail (Sigma Aldrich). Fifty micrograms of proteins for each sample were loaded into 10% sodium dodecyl sulfate polyacrylamide gel. After transfer to nitrocellulose membrane, blots were blocked with Tris-buffered saline-0.1% Tween 20 containing 5% bovine serum albumin (Sigma Aldrich) for 1 hour at room temperature, followed by incubation with primary antibody overnight at 4°C. The primary antibody was the same rabbit polyclonal anti-pccb antibody used for IHC (abcam ab96729). A mouse anti-β-actin antibody was used for normalization (Novus Biological). Anti-rabbit IgG-HRP or anti-mouse IgG-HRP (GE Healthcare) were used as secondary antibodies for detection and the blot were visualized using chemiluminescence.

Biochemical analysis

Larval cranial halves were pooled and lysed in PBS by tissue lyser. After centrifugation at 13,200 revolutions per minute for 15 min the supernatant was used for measurement of protein concentration and acylcarnitine analysis by tandem mass spectrometry performed by the MGL Laboratory at Baylor College of Medicine (Houston, Texas, US). Caudal halves were used to confirm the genotype, as described above.

Behavioral analysis

Live video tracking of medaka larvae was performed using DanioVision system (Noldus Information Technology, Leesburg, VA). 12 to 14 days post fertilization (dpf) larvae were chosen for this analysis because at this stage the abnormal phenotype was evident in almost all homozygous animals and this allowed their selection. Larvae were placed into 96-well plates, each well containing 150 µl of raising water, and introduced into the DanioVision observation chamber. The chamber includes an infra-red sensitive camera, a programmable white light source and a camera lens for an optimal image of all wells without angular distortion. Locomotor activity was evaluated after a 10-min acclimatization period to reduce anxiety-like behaviour. The EthoVision XT Software was used to analyze video tracks [78]. The thresholds for movement detection were 0.2 mm/s (start velocity) and 0.1 mm/s (stop velocity). For basal movement analysis, larvae were tracked over a 20-min light period and tracks were analyzed for total distance moved (mm) and movement cumulative duration (s). For analysis of motor response after light stimulation, larvae were kept in total darkness for 20 min before stimulation with the maximum light intensity. Movement parameters were measured over the 60 s following the light stimulation.

Treatments on affected larvae

Glucose and drugs were all added to the raising water. Larvae were raised in 6-well plates, and the water was changed every day. Treatments were performed since hatching. With the exception of the experiments with the low-protein diets, larvae were fed with standard fish food (Tetramin, Tetra, Spectrum Brands Company). The low protein diets containing either 15% or 30% of proteins were custom-made and provided by the USDA Agricultural Research Service, Bozeman, MT, USA. For all drugs, scalar concentrations were first administered to wt larvae to establish the maximum tolerated concentration in the absence of toxicity. The maximum tolerated concentration was used for treatment of PA larvae. The final concentration was 1 mM for antipyrine, 10 µM for carnitine, ornithine α-ketoglutarate (OKG) and sodium citrate, and 1 µM for glutamine. Antipyrine, carnitine, glutamine, and sodium citrate were all purchased by Sigma-Aldrich, and OKG from Bulkpowders. For survival analysis, larvae were all raised until 30 dpf; at dpf 30 all larvae were sacrificed and the cumulative survival during the observation period was calculated.

Drug screening

Movement analysis performed with the DanioVision system was used as first-line screening test. Total distance moved and movement cumulative duration were used as read-outs. The analysis was performed both in basal conditions (20 min) and after light stimulation (1 min). Larvae were placed in 96-well plates: 80 wells out of 96 contained *pccb*$^{del/del}$ larvae used to test 80 different compounds. Compounds were added to the raising medium at 10 µM concentration and robotically dispensed into single wells. The remaining 16 wells in each plate contained only raising medium, and were used as internal controls: 8 with wt larvae (positive controls) and 8 with non-treated *pccb*$^{del/del}$

larvae (negative control). Each plate was analyzed in triplicate. Movement analysis on a larger number of larvae (≥8) was performed as second-line screening. Hits passing the second-line screening were evaluated for their effect on survival.

For hits selection, I compared movement parameters between larvae treated with the investigational compounds and untreated larvae (negative controls). To this aim, for each compound I used results obtained from three independent experiments on single larvae. To pool results, I first normalized values from each plate on the basis of mean values from positive and negative controls. For each compound, means of normalized values obtained from the three experiments were compared with the mean of negative controls by 1-sided T-test. Those compounds showing significant improvement ($p<0.05$) for at least one movement parameter (compared to untreated *pccb*$^{del/del}$ larvae) were identified as potential hits.

Statistical analyses

T-test and the Fisher's exact test were used for comparisons between two experimental groups and two proportions, respectively. For Kaplan-Meier survival analysis, the Log rank Mantel-Cox test was applied. Outliers defined by two-sided Iglewicz and Hoaglin's robust test for multiple outliers (modified Z-score: 3.5) were excluded in behavioral analyses.

Results

Generation of PA medaka

To evaluate the presence of TALEN-induced mutations, I analyzed the target region in medaka larvae deriving from injected embryos.

I found no mutations in medaka larvae deriving from embryos injected with the *pcca* TALEN. To explain the lack of TALEN-induced mutations, I sequenced the genomic DNA extracted from our medaka colony and I detected a synonymous nucleotide change (c.204C>T) in the L recognition sequence of the TALEN on the *pcca* gene. This nucleotide change is likely responsible for the lack of recognition and TALEN-induced mutations.

In contrast to *pcca*, TALEN-induced mutations were found in 8/28 (~28%) larvae from *pccb* TALEN-injected embryos. As expected, I observed multiple mutations in a mosaic fashion, starting from position 390 (spacer sequence) (**Figure 3A**).

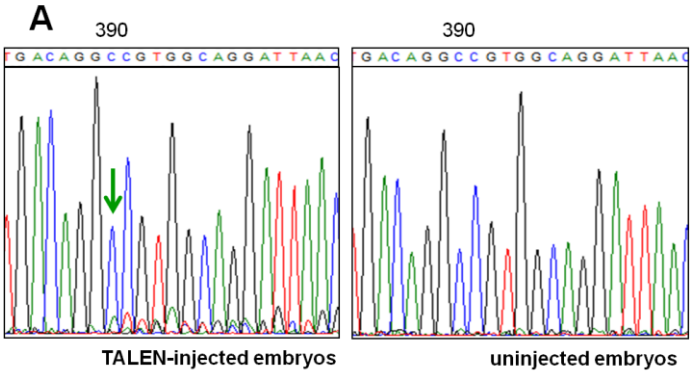

B

TGGTGACAGGCCGTGGCAGGATTAACGGCAGGCT	**wt**
TGGTGACAGGC - - - - - - AGGATTAACGGCAGGCT	**c.391_396delCGTGGC**
TGGTGACAGGCCGTTGGCAGGATTAACGGCAGGCT	**c.393dupT**
TGGTGACAGGCCGGTGGCAGGATTAACGGCAGGCT	**c.392dupG**
TGGTGACAGGC-AGGTGGCAGGATTAACGGCAGGCT	**c.[391delC];[391insAG]**
TGGTGACAGG - - - - - - - - - - ATTAACGGCAGGCT	**c.390_399delCCGTGGCAGG**
TGGTGACAGGCC - - - - - AGGATTAACGGCAGGCT	**c.392_396delGTGGC**
TGGTGACAGGCCGTGGCCGTGGCAGGATTAACGGCAGGCT	**c.391_396dupCGTGGC**
TGGTGACAGGCCG - - GCAGGATTAACGGCAGGCT	**c.393_394delTG**
TGGTGACAGGCCGTTGGGCAGGATTAACGGCAGGCT	**c.393dupTG**
TGGTGACAGGCC – TGGCAGGATTAACGGCAGGCT	**c.392delG**

Figure 3. (**A**) *On the left*: starting from nucleotide position 390 of *pccb* cDNA, the presence of multiple peaks underneath the predominant wt sequence (green arrow) suggests TALEN-induced mosaicism. *On the right*: multiple peaks are not visible in wt embryos. (**B).** TALEN induced mutations (indels) detected in larvae by targeting the exon 3 of the *pccb* medaka gene; inserted and duplicated bases are shown in red.

Germline transmission was not detected in 5/16 of G0 fishes deriving from TALEN-injected embryos (31.2%). For fishes showing germline transmission, the percentage of the offspring carrying *pccb* mutations ranged from 5% to 40%.

The analysis of *pccb* target sequences from G1 heterozygous fishes revealed 10 TALEN-induced mutations, the most frequent being an in-frame 6-bp deletion (c.391_396delCGTGGC) that is predicted to result in loss of two amino acids (R131-G132). There was only one other in-frame mutation (a duplication affecting the same base pairs: c.391_396dupCGTGGC) whereas all the others were frameshift insertions or deletions (**Figure 3B**).

The amino acids involved in the 6-bp deletion (R131-G132) are conserved in the human *PCCB* gene. Missense and nonsense mutations affecting corresponding amino acid residues in the human PCCB protein (R111-G112) have been reported in patients with early onset PA [13, 79, 80]. I hypothesized that the in-frame deletion could result in a less severe phenotype compared to frameshift mutations. Based on these considerations, I selected G1 heterozygous fishes bearing the c.391_396delCGTGGC mutation for future studies and therefore they were mated to generate $pccb^{del/del}$ larvae.

Phenotyping of $pccb^{del/del}$ medaka

I evaluated pccb protein levels by western blot and IHC on homozygous larvae, and I observed that the protein was detected in $pccb^{del/del}$ larvae at levels that were similar to wt and heterozygous larvae (**Figure 4A-B-C**)

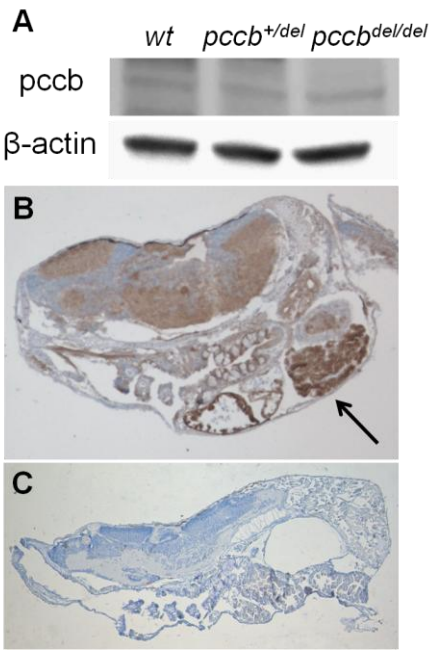

Figure 4. Pccb protein in *pccb*$^{del/del}$ larvae by western blot analysis on a pool of 18-20 larvae (**A**), and by pccb IHC on a sagittal section of a *pccb*$^{del/del}$ larva (**B**), that shows ubiquitous expression of the protein and increased signal in the liver (arrow). A negative control (no secondary antibody) is shown in (**C**). IHC in B and C are representative images of at least $N = 3$.

Homozygous *pccb*$^{del/del}$ larvae have a delayed mean hatching time (9.8 vs. 8.2 dpf of wt larvae), suggesting delayed embryonal development and/or reduction of prenatal motility (**Figure 5**).

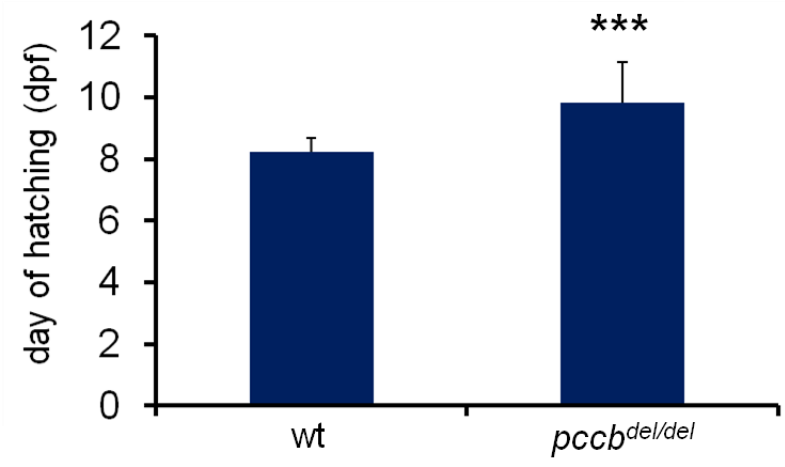

Figure 5. Mean hatching time in homozygous larvae compared to wt. Mean±SD; wt: $N = 30$, *pccb*$^{del/del}$: $N = 47$; ***p < 0.001; T-test.

No remarkable differences in the gross appearance were observed in *pccb*$^{del/del}$ larvae compared with wt larvae with the exception of yolk oedema suggesting inefficient reabsorption (**Figure 6**). The body and head size were mildly reduced, resembling growth failure observed in children with PA (**Figure 7A-B**).

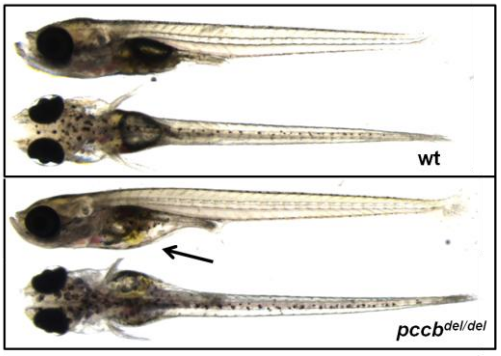

Figure 6. External appearance of 14-dpf larvae. The yolk oedema is shown by the arrow.

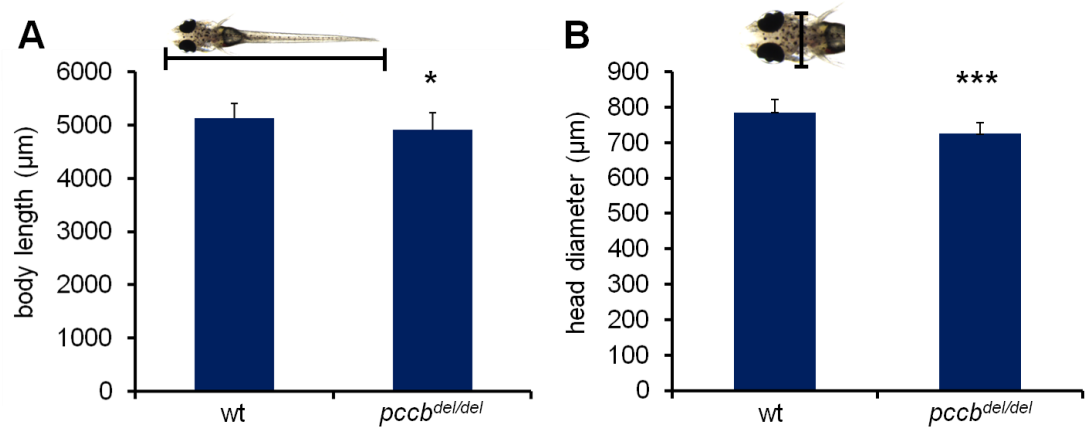

Figure 7. Body length (**A**) and head diameter (**B**) of *pccb*$^{del/del}$ larvae compared with wt. Mean±SD; *N*=23 for each group; *p<0.05, ***p<0.001; T-test.

Although cardiomyopathy is observed in human patients, no cardiac enlargement was detected in *pccb*$^{del/del}$ larvae and only a mild increase in the heart rate was detected (**Figure 8A-B**).

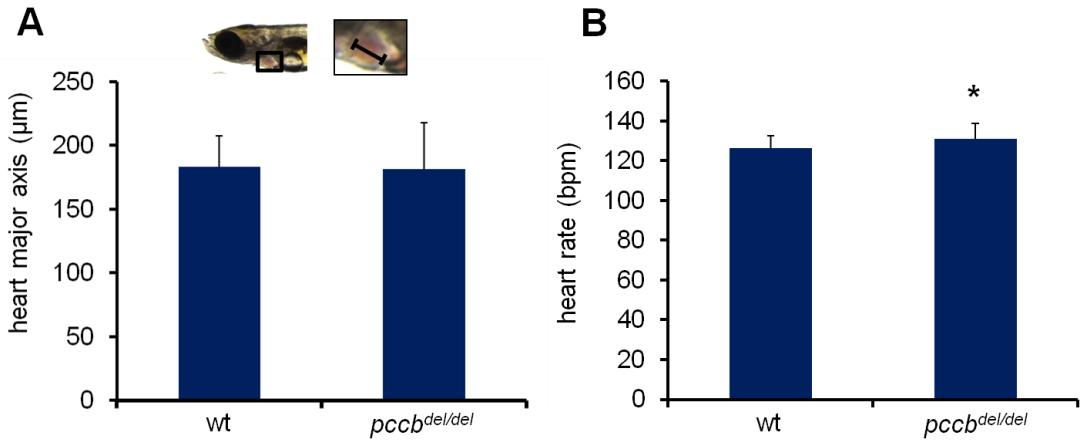

Figure 8. (**A**) Heart major axis was measured using stereomicroscope and used as marker of heart volume: no difference was observed between *pccb*$^{del/del}$ and wt larvae. Mean±SD; wt: *N* = 17, *pccb*$^{del/del}$: *N* = 16. (**B**) A mild increase in heart rate was observed in *pccb*$^{del/del}$ larvae. Mean±SD; wt: *N* = 23, *pccb*$^{del/del}$: *N* = 22; *p<0.05; T-test.

Most severely affected *pccb*$^{del/del}$ larvae showed reduced movements since hatching and death in the first days after hatching. Nevertheless, the majority of them presented normal at hatching and usually within 7 days from hatching, they showed abnormal movements and progressive loss of motility, inability to feed and lethargic state with complete lack of activity despite detectable heart beating. Abnormal movements such as "corkscrew" movements suggesting neurological impairment were also observed before progression of the disease to paralysis. All *pccb*$^{del/del}$ larvae did not survive beyond 20 days after hatching whereas less than 5% mortality was observed in heterozygous and wt larvae, consistent with previous data in medaka [81] (**Figure 9**).

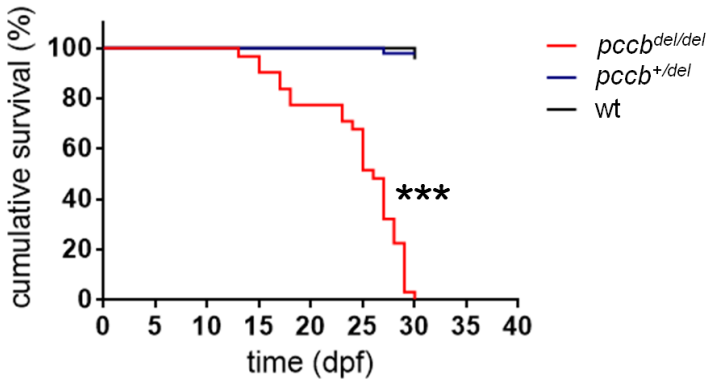

Figure 9. Kaplan-Meyer survival curve. Homozygous larvae have reduced survival compared to heterozygous and wt controls. Wt: *N* = 23, *pccb*+/-: *N* = 49, *pccb*$^{del/del}$: *N* = 31; ***p < 0.001; Mantel-Cox Log rank test.

Similar to PA patients, *pccb*$^{del/del}$ larvae did not show any organ malformations as determined by microscopic examination of living larvae and by H&E staining performed on a total of 25 larvae (12 wt, 13 *pccb*$^{del/del}$) (**Figure 10**).

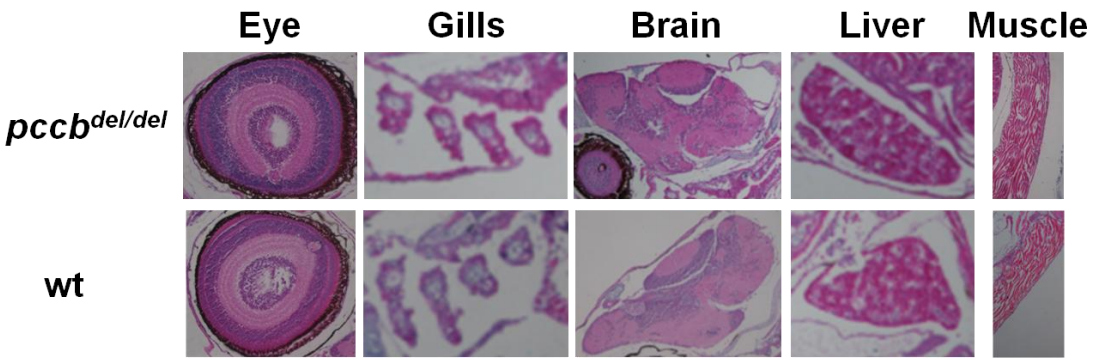

Figure 10. Hematoxylin-eosin staining on *pccb*$^{del/del}$ and wt larvae. No abnormalities were detected in *pccb*$^{del/del}$ compared to wt larvae.

Since fatty degeneration of the liver has been described in several historical reports of patients with PA [2, 37, 82] and presence of lipid droplets has been observed in the livers of the *Pcca* knockout mouse model of PA [55], I investigated lipid accumulation in *pccb*$^{del/del}$ medaka larvae by Oil Red staining. I observed lipid droplets in the liver of

10/14 *pccb*$^{del/del}$ larvae compared to 1/10 of wt (p<0.01, Fisher's test) (**Figure 11A**). Moreover, I also observed lipid droplets in the heart of 8/10 affected larvae compared to 1/8 wt (p<0.05, Fisher's test) (**Figure 11B**).

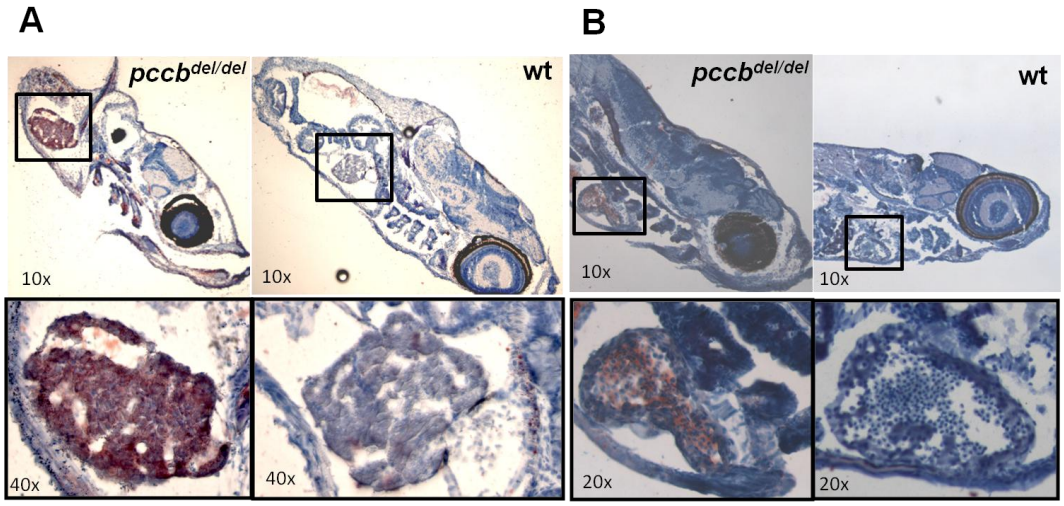

Figure 11. Oil Red staining showing lipid accumulation in the liver (**A**) and in the heart (**B**) of *pccb*$^{del/del}$ larvae, absent in almost all wt larvae.

Biochemical analysis

To investigate whether *pccb*$^{del/del}$ larvae recapitulate the biochemical abnormalities observed in PA patients, the acylcarnitine profiles on lysates obtained from pools of homozygous, heterozygous, and wt larvae were measured by tandem mass spectrometry. Homozygous larvae showed a significant increase in the levels of propionylcarnitine (C3), the major biochemical marker of the disease in human patients (**Figure 12**).

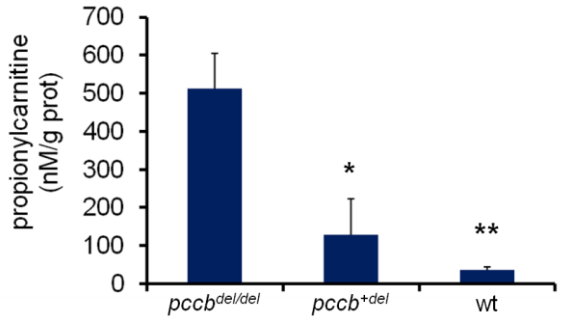

Figure 12. Propionylcarnitine levels in homozygous, heterozygous and wt larvae sacrificed at 11±3 dpf. Each sample is a lysate obtained from a pool composed of 18 larvae. Results are normalized for protein concentration. Mean±SD; *N* = 3; *p < 0.05; **p<0.01; T-test.

Behavioral phenotype

Affected larvae showed a locomotor defect that ranged from reduction to total lack of movements. Automated quantitative analysis of locomotor behavior confirmed significant deficiency in movements measured by two parameters (total distance moved and movement cumulative duration), during 20 minute-observations under basal conditions and 1 minute-observation after light stimulation (**Figure 13**). Although reduced compared to wt fishes, the presence of a startle reaction after light stimulation in *pccb*$^{del/del}$ larvae suggests some preservation of visual function.

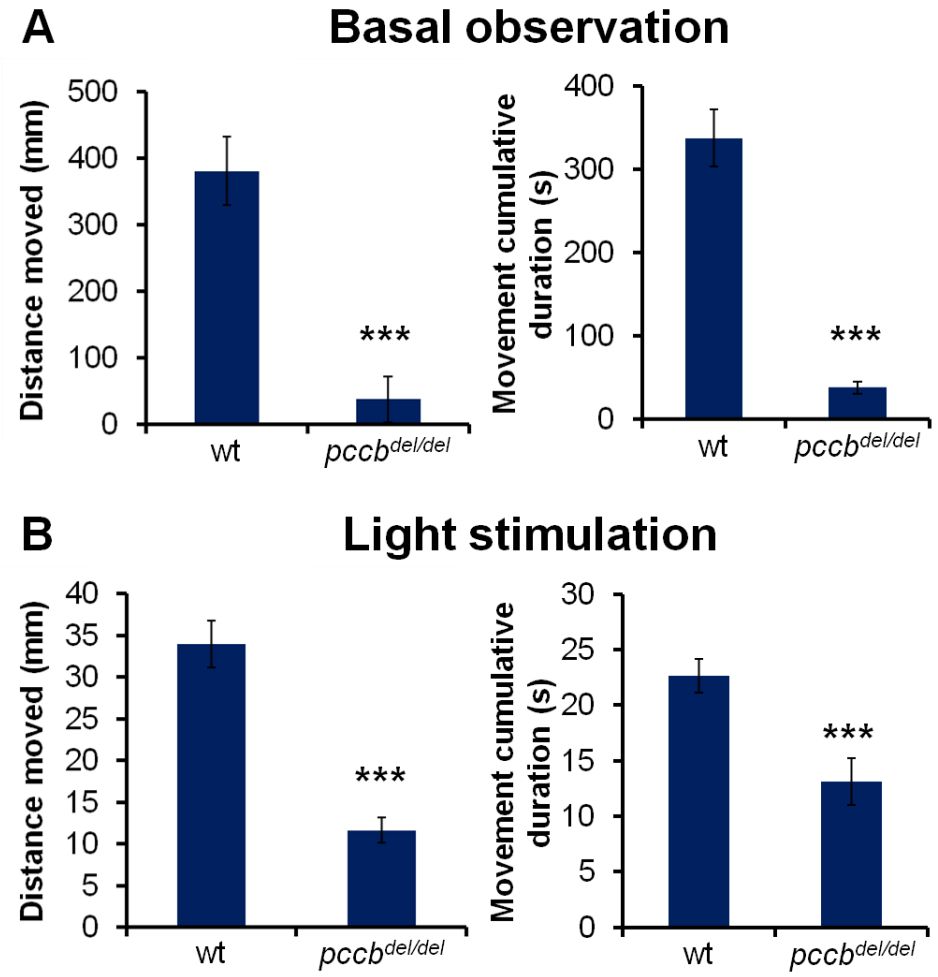

Figure 13. Movement analysis showing severe reduction of locomotor behavior in *pccb*$^{del/del}$ larvae compared to wt both under basal conditions (**A**) and after light stimulation (**B**). Mean±SE; basal observation: wt *N* = 28, *pccb*$^{del/del}$ *N* = 25; light stimulation: distance moved wt *N* = 31, *pccb*$^{del/del}$ *N* = 22, movement duration wt *N* = 31, *pccb*$^{del/del}$ *N* = 28; ***p<0.001; T-test.

Efficacy of low protein diet in PA fishes

I evaluated the response of PA larvae to a low protein diet aimed at reducing propionyl-CoA production. I compared two low protein diets with different protein content (15% and 30%, respectively). Larvae fed with the diet with the lowest protein content (15%) showed increased survival (**Figure 14**). This result suggests a toxic effect of food proteins, recapitulates a feature seen in PA patients, and supports the validity of *pccb*$^{del/del}$ medaka fishes as a disease animal model of PA.

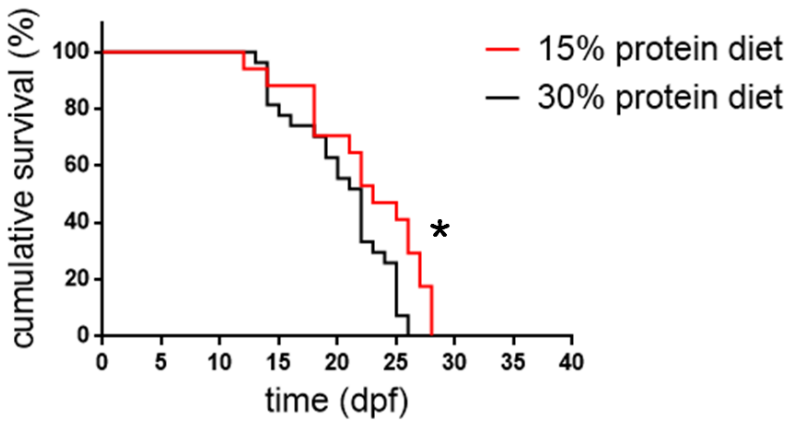

Figure 14. PA larvae fed with higher protein concentration showed increased mortality. Wt: *N* = 27, *pccb*$^{del/del}$: *N* = 17; *p<0.05; Mantel-Cox Log rank test.

Efficacy of anaplerotic therapy in PA fishes

Anaplerotic therapy is a treatment aimed at improving energy metabolism by replenishing Krebs cycle metabolites. Anaplerotic therapy in PA patients has been proposed [33]. However, there are no evidences either in clinical or preclinical studies supporting its efficacy for therapy of PA. Therefore, I investigated an anaplerotic therapy composed of sodium citrate, OKG and glutamine in *pccb*$^{del/del}$ fishes. The anaplerotic therapy was administered either alone or in combination with carnitine (the drug given to PA patients to increase propionic acid excretion) and glucose (as a non-protein source of energy). In both cases, larvae treated with the anaplerotic therapy showed a significant improvement of survival (**Figure 15A-B**). Moreover, a significant

improvement in movement parameters was detected in larvae treated with anaplerotic therapy (**Figure 15C-D**).

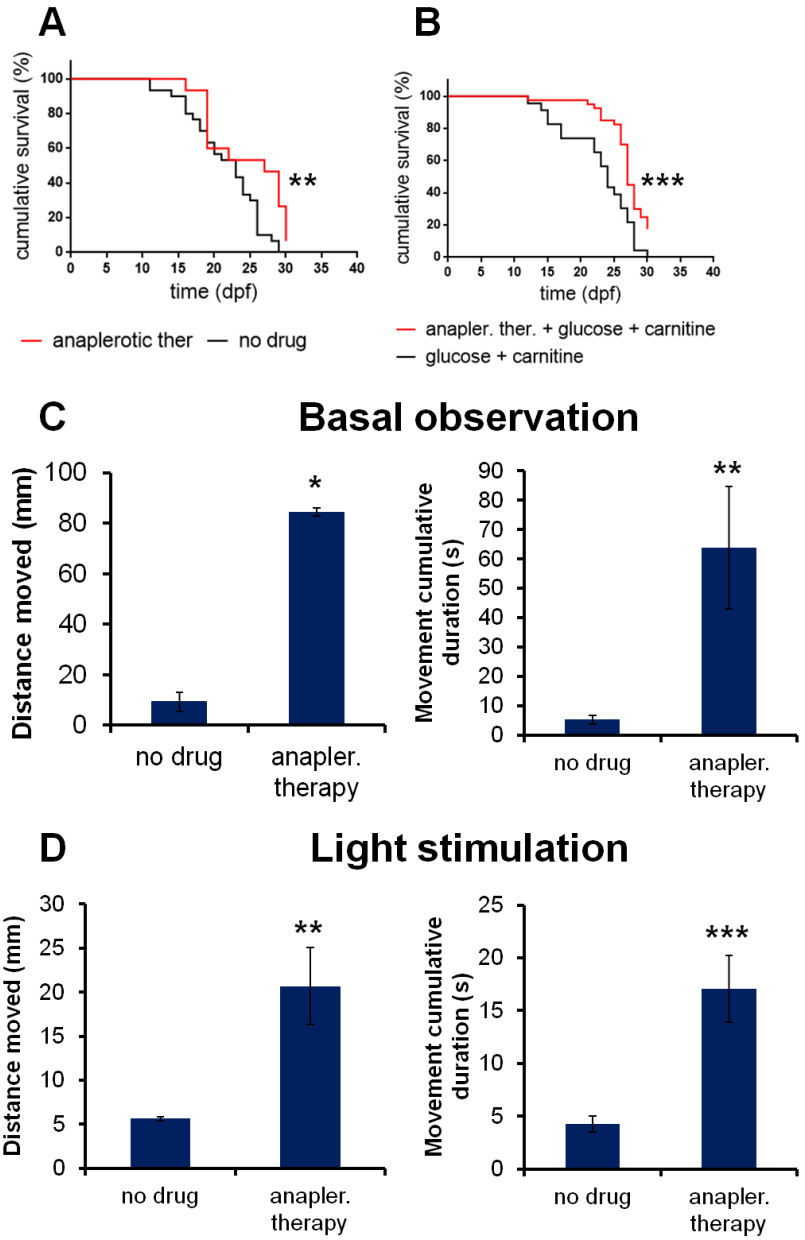

Figure 15. (**A**) *pccb*$^{del/del}$ larvae showed significant increased survival after administration of anaplerotic therapy. No drug: *N* = 30, anapl. ther.: *N*=15; **p<0.01; Mantel-Cox Log Rank test. (**B**) Anaplerotic therapy in combination with glucose and carnitine improved survival compared to glucose and carnitine. Glucose plus carnitine: *N* = 23, anapl. ther. plus glucose and carnitine: *N* =40; ***p<0.001; Mantel-Cox Log rank test. (**C-D**) *pccb*$^{del/del}$ larvae treated with anaplerotic therapy showed significant increase in locomotor activity both under basal conditions (**C**) and after light stimulation (**D**). Mean±SE; no drug: *N* = 5, anapl. ther.: *N* = 13; *p<0.05**p<0.01; ***p<0.001; T-test.

High throughput drug screening in pccb$^{del/del}$ fishes

The PA medaka model is a suitable animal model for large-scale drug screening. With the goal of performing a high throughput drug screening in *pccb*$^{del/del}$ fishes, I set up the assay for the screening and began the evaluation of a subset of drugs from the Prestwick Library that is composed of 1280 Food and Drug Administration (FDA)-approved drugs. The preliminary screening was performed on the first plate (80 compounds).

After the first-line screening, I identified 14 positive hits that correspond to compounds that improved at least one movement parameter compared to negative controls (untreated larvae). To avoid false positive hits, I performed the screening in triplicate and I selected drugs that showed efficacy in all three experiments. In the initial screening three compounds (antipyrine; dapsone; sulpiride) were found positive and were evaluated for the second-line screening in a larger number of larvae (≥8) (**Figure 16**). The improvement by sulpiride and dapsone was not confirmed on the second-line screening whereas antypyrine was confirmed to be effective at improving the movement behaviour.

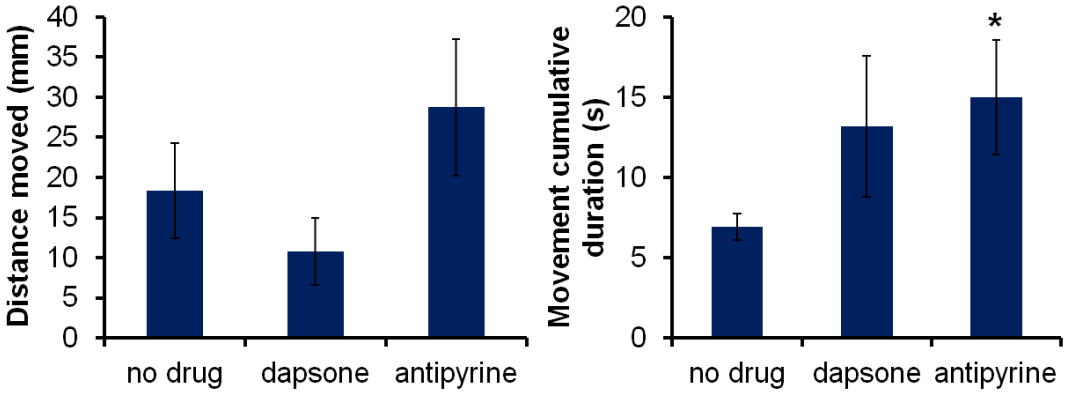

Figure 16. Second-line screening by movement analysis over a 20-min observation period in basal conditions. *pccb*$^{del/del}$ larvae incubated with antipyrine showed improvement in one parameter. Mean±SE; no drug: $N = 8$, dapsone: $N = 9$, antipyrine $N = 8$; *$p<0.05$; T-test.

Finally, I evaluated survival of larvae treated with antipyrine, but I did not observe a significant improvement in treated larvae compared to untreated (**Figure 17**). Therefore, the antipyrine does not appear to affect the natural progression of the disease in fishes.

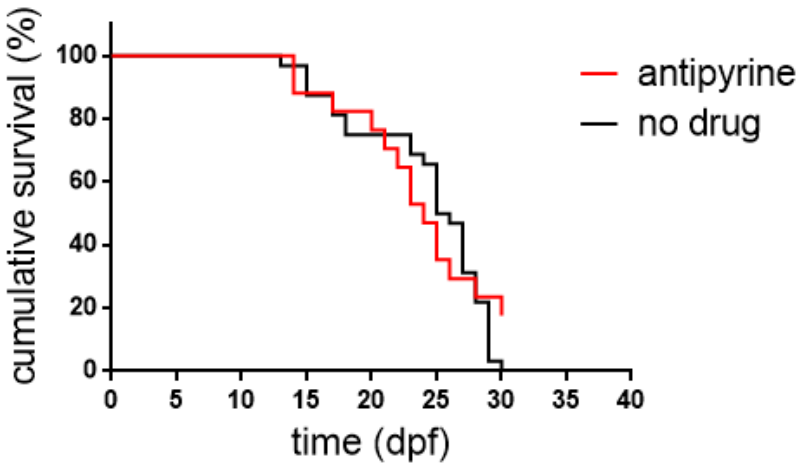

Figure 17. No improvement in survival was observed in *pccb*$^{del/del}$ larvae treated with antipyrine, compared to wt. No drug: *N* = 31, antipyrine: *N* = 19.

Discussion

PA is a severe disease presenting with life-threatening metabolic decompensations and multi-organ involvement. Effective therapies are still not available and patients continue to be at risk of developing lethal metabolic crisis and invalidating complications.

The available mouse model is a valuable tool for investigating experimental therapies. However, it is not suitable for large drug screening.

An ideal treatment for PA should be sufficiently safe and ready to be administered in the newborn period or even prenatally if a prenatal diagnosis of PA is made. Moreover, it should be effective in correcting disease manifestations in different organs. A high-throughput drug screening is an attractive approach to rapidly investigate a large number of drugs *in vivo*. The small fishes give the unique possibility to perform such an *in vivo* high-throughput drug screening. Therefore, for this thesis project I generated a medaka model of PA and set the conditions for the use of this model for therapeutic investigations and drug screening.

To generate knock-out fishes, I used TALEN technology, a genome editing strategy with high efficacy and specificity for the targeted region. Among the embryos targeted in *pccb*, I chose those bearing the in-frame deletion with higher chances to result in a non-lethal phenotype. The deletion involves the residues R131-G132 of the pccb protein and by comparison with the human PCCB sequence these residues (corresponding to human R111-G112 amino acids) are located in a conserved region.

Based on the analysis performed by Huang et al. on the bacterial PCC, the G112D mutation described in PA patients was located in the β-subunit in a region near to the interface with the α-subunit, and the amino acid change was thought to determine

disruption of the β-subunit integrity because of the introduction of the aspartate side chain [12]. Indeed, human fibroblasts with the G112D mutation showed almost undetectable PCC activity and reduced to absent Pccb protein, in the presence of normal mRNA levels [13, 83]. In *pccb*$^{del/del}$ fishes I observed levels of pccb protein comparable to wt, indicating that the mutant protein is stable and not subjected to early degradation. On the basis of the structural characterization of the protein I can therefore hypothesize that the amino acids deletion, located in a region near the interface with the α-subunit, could hamper the interaction with the α-subunit, without disrupting the integrity of the β-subunit.

Patients with PA are usually normal at birth and the disease only manifests in the postnatal period. In contrast, affected larvae showed a delay in the hatching time that may suggest an impaired embryonal development. Early onset of energy deficiency leading to movement impairment may be the result of early accumulation of toxic metabolites. Compared to the intrauterine prenatal development of humans, medaka have an external embryo development and residual maternal RNA does not last more than 48-72 h post fertilization. Therefore, medaka might suffer from the toxic effects of PA metabolites at earlier stages.

The phenotype of *pccb*$^{del/del}$ larvae resembles the severe early-onset PA. Untreated children with early-onset PA have 100% mortality in the first years of life. PA patients are substantially normal in their appearance, except for possible growth failure and microcephaly. Similarly, affected larvae did not show organ malformations or gross differences in external appearance, but only very mild reduction in their mean body length and head diameter. The reduced growth was observed in the first days after hatching, and thus, it is not the result of impaired feeding. Affected larvae showed yolk retention, an indicator of development delay and a known sign of toxicity in both medaka and zebrafish. According to some authors it is a sign of liver toxicity [84-86].

Fatty degeneration of the liver has been described since the first reports in patients with severe PA [2, 37, 82]. Hypothesis explaining this finding include inhibition of fatty acids β-oxidation due to toxic metabolites and increased synthesis of odd-chain fatty acids. Indeed, impaired oxidation of ^{14}C-palmitate by propionic acid has been observed [27] and could be due both to direct enzyme inhibition by toxic metabolites and reduced carnitine and free acyl-CoA pool. On the other hand, propionyl-CoA acts as a primer for odd-chain fatty acid synthesis and increased amount of odd-numbered long chain fatty acids has been observed in erythrocytes from patients with PA [87]. Lipid droplets have been also observed in the liver of the *Pcca* knockout mouse model of PA [55] and reduced expression of β oxidation enzyme hydroxyacyl-coa dehydrogenase has been detected in liver, muscle, and heart of the *Pcca-/-* mouse [38]. Consistent with these data, I observed presence of lipid droplets in *pccb*$^{del/del}$ larvae. Increased lipid staining was also present in the heart. This is consistent with the high β-oxidation activity of the heart. However, no alterations of heart volume and morphology were detected in *pccb*$^{del/del}$ larvae. A very mild increase in the heart rate is a rather non-specific sign.

The markedly increased levels of propionylcarnitine which is the biochemical hallmark of the disease, makes the medaka model similar to humans and supports the validity of the fish as a disease model. Further confirmation for the validity of the model came from the response to low protein diet that improved survival.

CNS is one major organ affected in PA and almost all patients have some degree of neurological or cognitive impairment. The locomotor activity in small fishes reflects their neurologic status. Homozygous larvae indeed showed signs of neurological impairment such as severe reduction of movements and abnormal movements like “corkscrew” swimming, suggesting a seizure phenotype [88]. The progression towards a lethargic state preceding death also resembles the late evolution of the PA phenotype in untreated neonatal-onset patients.

Once the PA medaka fishes were generated, I used them to investigate a specific therapy and to validate them for high-throughput drug screening.

The metabolic derangement underlying PA is the result of both accumulation of toxic metabolites and impaired energy metabolism due to depletion of Krebs cycle intermediates and inhibition of mitochondrial electron transport chain. Anaplerotic therapy is aimed at providing substrates to the Krebs cycle. Triheptanoin, an odd-carbon triglyceride, has been administered as precursor of acetyl-CoA and propionyl-CoA in patients with pyruvate carboxylase deficiency, carnitine palmitoyltransferase II deficiency and long-chain fatty acids oxidation defects, with good clinical outcomes [89-92]. Administration of PA precursors will worsen PA but anaplerotic therapy supplying Krebs cycle intermediates and their precursors has potential to be effective. PA indeed results in Krebs cycle impairment due to enzyme inhibition and depletion of intermediates, as well as depletion of the glutamate/glutamine pool. Therefore supplementation with α-ketoglutarate and sodium citrate plus glutamine could improve the Krebs cycle (**Figure 18**) [33].

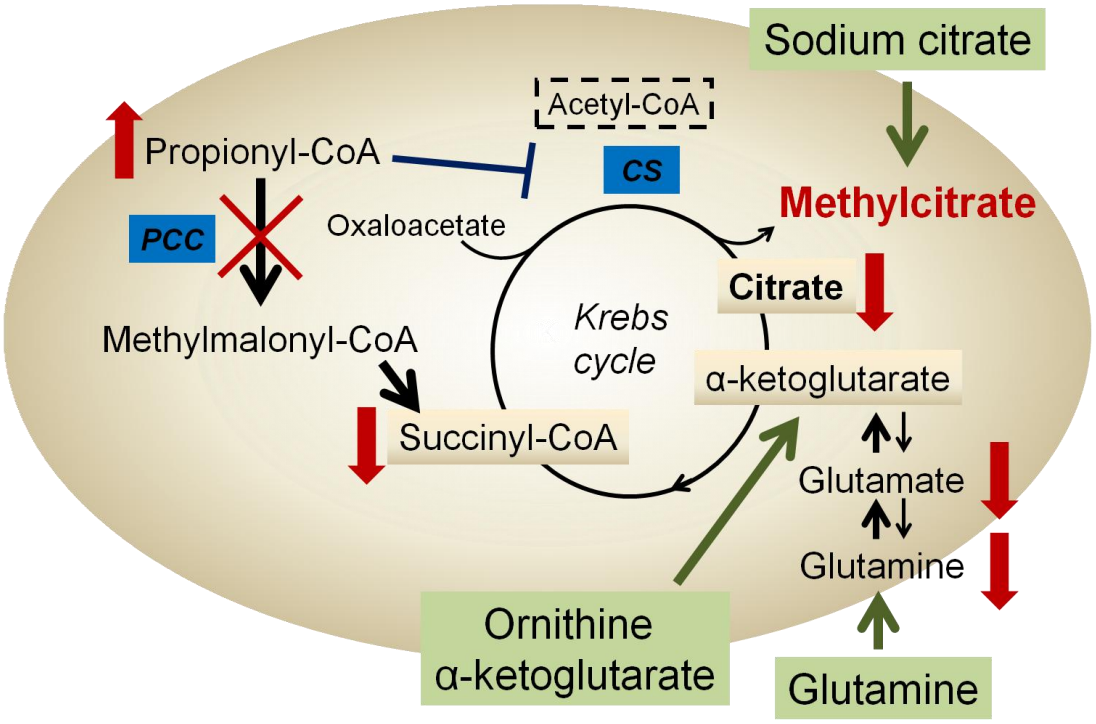

Figure 18. Schematic representation of the rationale for the anaplerotic therapy in PA. Krebs cycle impairment is caused by deficient production of succinyl-CoA and citrate, as well as direct inhibition of several enzymes. To provide α-ketoglutarate to the Krebs cycle, reactions catalyzed by glutamate dehydrogenase and glutaminase are shifted towards deamination of glutamate and glutamine, with depletion of the glutamate/glutamine pool. Administration of ornithine-α-ketoglutarate, glutamine and sodium citrate (in green) could contribute to replenish the Krebs cycle, improve energy production and reduce catabolism.

Because a detrimental consequence of energy deficiency in PA is the lack of ATP production leading to activation of catabolic pathways (likely through AMP kinase) that in turn causes further production of toxic metabolites, it can be hypothesized that inducing a shift towards anabolism would be beneficial [89]. For this reason, ornithine was administered together with α-ketoglutarate with the goal of stimulating anabolism. Ornithine is conjugated in form of salt to α-ketoglutarate (OKG), in a 2:1 molar ratio, because it has been demonstrated that the simultaneous administration of these two metabolites in this ratio shifts the metabolism of ornithine towards arginine formation, providing an important stimulus to anabolism [93]. OKG has been used for years in patients with several conditions for its beneficial actions on nutritional status, wound healing and immune system [93]. Although the use of anaplerotic therapy has been proposed for several years [33], its efficacy has never been proved neither in human patients with PA nor in animal models.

The anaplerotic therapy significantly improved both survival and locomotor behaviour of PA larvae, suggesting that it is a promising therapy for PA.

Finally, I set up a screening assay for drug discovery in the PA medaka model and I evaluated the first 80 compounds of the Prestwick Library. The use of whole animals for screening and locomotor behaviour as read-out have the advantage of overcoming the *in vitro* analyses and to immediately test drugs based on their effect on clinically relevant endpoints. One limitation of this analysis is the variability in movement

parameters in affected larvae. However, performing the first-line screening in triplicate and the second-line screening on a larger number of larvae can overcome this limitation. After a first-line screening on a limited number of compounds, I selected three potential hits, and one of them (antipyrine) was confirmed in the second-line screening, resulting in a mild effect on movement. This drug did not result in effects on survival and therefore did not affect the natural history of the disorder. Nevertheless, it may still be an effective treatment that might lead to some degree of amelioration and requires further investigation. Finally, I have set the conditions for the screening of the whole drug library. The use of the Prestwick Library composed of FDA-approved drugs has the advantage of being rapidly transferred to the bedside without the need of expensive and time-consuming toxicity studies.

In summary, I generated a medaka model of PA that recapitulates the main clinical and biochemical features of the disease and is a valuable tool for therapeutic investigation. I have tested the efficacy of anaplerotic therapy, a treatment with high potential for clinical translation and I have set the conditions for a high-throughput drug screening on whole animals that could lead to the identification of effective drugs for therapy of PA.

Acknowledgements

I would like to acknowledge:

- Prof. Jonathan Gitlin (Marine Biological Laboratory, Woods Hole, Massachussets, US), for supervision and scientific advice;
- Dr. Elena De Felice (Nicola Brunetti-Pierri's Lab at TIGEM) for collaboration on the project;
- Dr. Ivan Conte and Francesco G. Salierno (Medaka facility at TIGEM) for scientific advice and collaboration on the project;
- Dr. Diego Medina and Dr. Luca G. Wanderlingh (High-content screening facility at TIGEM) for collaboration on drug screening;
- Dr. Paolo Sordino and Dr. Rosa Sepe (Stazione Zoologica Anton Dohrn, Naples, Italy) for collaboration on behavioral analysis;
- Dr. Rick Barrows (USDA Agricultural Research Service, Bozeman, Montana, USA) for providing low protein diets.

References

1. Childs, B., et al., *Idiopathic hyperglycinemia and hyperglycinuria: a new disorder of amino acid metabolism. I.* Pediatrics, 1961. **27**: p. 522-38.
2. Hommes, F.A., et al., *Propionicacidemia, a new inborn error of metabolism.* Pediatr Res, 1968. **2**(6): p. 519-24.
3. Hsia, Y.E., K.J. Scully, and L.E. Rosenberg, *Inherited propionyl-Coa carboxylase deficiency in "ketotic hyperglycinemia".* J Clin Invest, 1971. **50**(1): p. 127-30.
4. Gompertz, D., et al., *Localisation of enzymic defect in propionicacidaemia.* Lancet, 1970. **1**(7657): p. 1140-3.
5. Carrillo-Carrasco, N. and C. Venditti, *Propionic Acidemia*, in *GeneReviews(R)*, R.A. Pagon, et al., Editors. 1993: Seattle (WA).
6. Chapman, K.A. and M.L. Summar, *Propionic acidemia consensus conference summary.* Mol Genet Metab, 2012. **105**(1): p. 3-4.
7. Ravn, K., et al., *High incidence of propionic acidemia in greenland is due to a prevalent mutation, 1540insCCC, in the gene for the beta-subunit of propionyl CoA carboxylase.* Am J Hum Genet, 2000. **67**(1): p. 203-6.
8. Yorifuji, T., et al., *Unexpectedly high prevalence of the mild form of propionic acidemia in Japan: presence of a common mutation and possible clinical implications.* Hum Genet, 2002. **111**(2): p. 161-5.
9. Rashed, M.S., *Clinical applications of tandem mass spectrometry: ten years of diagnosis and screening for inherited metabolic diseases.* J Chromatogr B Biomed Sci Appl, 2001. **758**(1): p. 27-48.
10. Fenton, W.A., R.A. Gravel, and D.S. Rosenblatt, *Organic Acids – Disorders of Propionate and Methylmalonate metabolism.*, in *The Online Metabolic and*

Molecular Bases of Inherited Disease, M. David Valle, Editor-in-Chief, Arthur L. Beaudet, MD, Editor, Bert Vogelstein, MD, Editor, Kenneth W. Kinzler, Ph.D., Editor, Stylianos E. Antonarakis, MD, D.Sc., Editor, Andrea Ballabio, MD, Editor, K. Michael Gibson, Ph.D., FACMG, Editor, Grant Mitchell, MD, Editor, (McGraw-Hill Medical), Editor. 2001. p. 2165-2193.

11. Leonard, J.V., *Stable isotope studies in propionic and methylmalonic acidaemia.* Eur J Pediatr, 1997. **156 Suppl 1**: p. S67-9.
12. Huang, C.S., et al., *Crystal structure of the alpha(6)beta(6) holoenzyme of propionyl-coenzyme A carboxylase.* Nature, 2010. **466**(7309): p. 1001-5.
13. Perez, B., et al., *Propionic acidemia: identification of twenty-four novel mutations in Europe and North America.* Mol Genet Metab, 2003. **78**(1): p. 59-67.
14. Desviat, L.R., et al., *Propionic acidemia: mutation update and functional and structural effects of the variant alleles.* Mol Genet Metab, 2004. **83**(1-2): p. 28-37.
15. Kraus, J.P., et al., *Mutation analysis in 54 propionic acidemia patients.* J Inherit Metab Dis, 2012. **35**(1): p. 51-63.
16. Desviat, L.R., et al., *New splicing mutations in propionic acidemia.* J Hum Genet, 2006. **51**(11): p. 992-7.
17. Gallego-Villar, L., et al., *Functional characterization of novel genotypes and cellular oxidative stress studies in propionic acidemia.* J Inherit Metab Dis, 2013. **36**(5): p. 731-40.
18. Kolker, S., et al., *The phenotypic spectrum of organic acidurias and urea cycle disorders. Part 1: the initial presentation.* J Inherit Metab Dis, 2015. **38**(6): p. 1041-57.

19. Deodato, F., et al., *Methylmalonic and propionic aciduria.* Am J Med Genet C Semin Med Genet, 2006. **142C**(2): p. 104-12.

20. Grunert, S.C., et al., *Propionic acidemia: clinical course and outcome in 55 pediatric and adolescent patients.* Orphanet J Rare Dis, 2013. **8**: p. 6.

21. Karimzadeh, P., et al., *Propionic acidemia: diagnosis and neuroimaging findings of this neurometabolic disorder.* Iran J Child Neurol, 2014. **8**(1): p. 58-61.

22. Schreiber, J., et al., *Neurologic considerations in propionic acidemia.* Mol Genet Metab, 2012. **105**(1): p. 10-5.

23. Massoud, A.F. and J.V. Leonard, *Cardiomyopathy in propionic acidaemia.* Eur J Pediatr, 1993. **152**(5): p. 441-5.

24. Baumgartner, D., et al., *Prolonged QTc intervals and decreased left ventricular contractility in patients with propionic acidemia.* J Pediatr, 2007. **150**(2): p. 192-7, 197 e1.

25. Baruteau, J., et al., *Successful reversal of propionic acidaemia associated cardiomyopathy: evidence for low myocardial coenzyme Q10 status and secondary mitochondrial dysfunction as an underlying pathophysiological mechanism.* Mitochondrion, 2014. **17**: p. 150-6.

26. Pena, L., et al., *Natural history of propionic acidemia.* Mol Genet Metab, 2012. **105**(1): p. 5-9.

27. Glasgow, A.M. and H.P. Chase, *Effect of propionic acid on fatty acid oxidation and ureagenesis.* Pediatr Res, 1976. **10**(7): p. 683-6.

28. Hayasaka, K. and K. Tada, *Effects of the metabolites of the branched-chain amino acids and cysteamine on the glycine cleavage system.* Biochem Int, 1983. **6**(2): p. 225-30.

29. Coude, F.X., L. Sweetman, and W.L. Nyhan, *Inhibition by propionyl-coenzyme A of N-acetylglutamate synthetase in rat liver mitochondria. A possible explanation for hyperammonemia in propionic and methylmalonic acidemia.* J Clin Invest, 1979. **64**(6): p. 1544-51.

30. Tuchman, M. and M. Yudkoff, *Blood levels of ammonia and nitrogen scavenging amino acids in patients with inherited hyperammonemia.* Mol Genet Metab, 1999. **66**(1): p. 10-5.

31. Sauer, S.W., et al., *Intracerebral accumulation of glutaric and 3-hydroxyglutaric acids secondary to limited flux across the blood-brain barrier constitute a biochemical risk factor for neurodegeneration in glutaryl-CoA dehydrogenase deficiency.* J Neurochem, 2006. **97**(3): p. 899-910.

32. Schwab, M.A., et al., *Secondary mitochondrial dysfunction in propionic aciduria: a pathogenic role for endogenous mitochondrial toxins.* Biochem J, 2006. **398**(1): p. 107-12.

33. Filipowicz, H.R., et al., *Metabolic changes associated with hyperammonemia in patients with propionic acidemia.* Mol Genet Metab, 2006. **88**(2): p. 123-30.

34. Wajner, M. and S.I. Goodman, *Disruption of mitochondrial homeostasis in organic acidurias: insights from human and animal studies.* J Bioenerg Biomembr, 2011. **43**(1): p. 31-8.

35. de Keyzer, Y., et al., *Multiple OXPHOS deficiency in the liver, kidney, heart, and skeletal muscle of patients with methylmalonic aciduria and propionic aciduria.* Pediatr Res, 2009. **66**(1): p. 91-5.

36. Fragaki, K., et al., *Fatal heart failure associated with CoQ10 and multiple OXPHOS deficiency in a child with propionic acidemia.* Mitochondrion, 2011. **11**(3): p. 533-6.

37. Hayasaka, K., et al., *Comparison of cytosolic and mitochondrial enzyme alterations in the livers of propionic or methylmalonic acidemia: a reduction of cytochrome oxidase activity.* Tohoku J Exp Med, 1982. **137**(3): p. 329-34.

38. Gallego-Villar, L., et al., *In vivo evidence of mitochondrial dysfunction and altered redox homeostasis in a genetic mouse model of propionic acidemia: Implications for the pathophysiology of this disorder.* Free Radic Biol Med, 2016. **96**: p. 1-12.

39. Haas, R.H., et al., *Acute basal ganglia infarction in propionic acidemia.* J Child Neurol, 1995. **10**(1): p. 18-22.

40. Laemmle, A., et al., *Propionic acidemia in a previously healthy adolescent with acute onset of dilated cardiomyopathy.* Eur J Pediatr, 2014. **173**(7): p. 971-4.

41. Ballhausen, D., et al., *Evidence for catabolic pathway of propionate metabolism in CNS: expression pattern of methylmalonyl-CoA mutase and propionyl-CoA carboxylase alpha-subunit in developing and adult rat brain.* Neuroscience, 2009. **164**(2): p. 578-87.

42. Kolker, S., et al., *The aetiology of neurological complications of organic acidaemias--a role for the blood-brain barrier.* J Inherit Metab Dis, 2006. **29**(6): p. 701-4; discussion 705-6.

43. Rousson, R. and P. Guibaud, *Long term outcome of organic acidurias: survey of 105 French cases (1967-1983).* J Inherit Metab Dis, 1984. **7 Suppl 1**: p. 10-2.

44. Sass, J.O., et al., *Propionic acidemia revisited: a workshop report.* Clin Pediatr (Phila), 2004. **43**(9): p. 837-43.

45. Sutton, V.R., et al., *Chronic management and health supervision of individuals with propionic acidemia.* Mol Genet Metab, 2012. **105**(1): p. 26-33.

46. Baumgartner, M.R., et al., *Proposed guidelines for the diagnosis and management of methylmalonic and propionic acidemia.* Orphanet J Rare Dis, 2014. **9**: p. 130.

47. Ah Mew, N., et al., *N-carbamylglutamate augments ureagenesis and reduces ammonia and glutamine in propionic acidemia.* Pediatrics, 2010. **126**(1): p. e208-14.

48. Barshes, N.R., et al., *Evaluation and management of patients with propionic acidemia undergoing liver transplantation: a comprehensive review.* Pediatr Transplant, 2006. **10**(7): p. 773-81.

49. Vara, R., et al., *Liver transplantation for propionic acidemia in children.* Liver Transpl, 2011. **17**(6): p. 661-7.

50. Kok, C.Y., et al., *Adeno-associated virus-mediated rescue of neonatal lethality in argininosuccinate synthetase-deficient mice.* Mol Ther, 2013. **21**(10): p. 1823-31.

51. Wang, L., et al., *AAV8-mediated hepatic gene transfer in infant rhesus monkeys (Macaca mulatta).* Mol Ther, 2011. **19**(11): p. 2012-20.

52. Chandler, R.J., et al., *Vector design influences hepatic genotoxicity after adeno-associated virus gene therapy.* J Clin Invest, 2015. **125**(2): p. 870-80.

53. Reiss, J. and R. Hahnewald, *Molybdenum cofactor deficiency: Mutations in GPHN, MOCS1, and MOCS2.* Hum Mutat, 2011. **32**(1): p. 10-8.

54. Donsante, A., et al., *AAV vector integration sites in mouse hepatocellular carcinoma.* Science, 2007. **317**(5837): p. 477.

55. Miyazaki, T., et al., *Fatal propionic acidemia in mice lacking propionyl-CoA carboxylase and its rescue by postnatal, liver-specific supplementation via a transgene.* J Biol Chem, 2001. **276**(38): p. 35995-9.

56. Guenzel, A.J., et al., *Generation of a hypomorphic model of propionic acidemia amenable to gene therapy testing.* Mol Ther, 2013. **21**(7): p. 1316-23.

57. Guenzel, A.J., et al., *Effects of adeno-associated virus serotype and tissue-specific expression on circulating biomarkers of propionic acidemia.* Hum Gene Ther, 2014. **25**(9): p. 837-43.

58. Guenzel, A.J., et al., *Long-term sex-biased correction of circulating propionic acidemia disease markers by adeno-associated virus vectors.* Hum Gene Ther, 2015. **26**(3): p. 153-60.

59. Love, D.R., et al., *Technology for high-throughput screens: the present and future using zebrafish.* Curr Opin Biotechnol, 2004. **15**(6): p. 564-71.

60. Kokel, D., et al., *Rapid behavior-based identification of neuroactive small molecules in the zebrafish.* Nat Chem Biol, 2010. **6**(3): p. 231-237.

61. Mathias, J.R., M.T. Saxena, and J.S. Mumm, *Advances in zebrafish chemical screening technologies.* Future Med Chem, 2012. **4**(14): p. 1811-22.

62. Mendelsohn, B.A., et al., *Atp7a determines a hierarchy of copper metabolism essential for notochord development.* Cell Metab, 2006. **4**(2): p. 155-62.

63. Madsen, E.C. and J.D. Gitlin, *Zebrafish mutants calamity and catastrophe define critical pathways of gene-nutrient interactions in developmental copper metabolism.* PLoS Genet, 2008. **4**(11): p. e1000261.

64. Song, Y., et al., *Mechanisms underlying metabolic and neural defects in zebrafish and human multiple acyl-CoA dehydrogenase deficiency (MADD).* PLoS One, 2009. **4**(12): p. e8329.

65. Friedrich, T., et al., *Mutation of zebrafish dihydrolipoamide branched-chain transacylase E2 results in motor dysfunction and models maple syrup urine disease.* Dis Model Mech, 2012. **5**(2): p. 248-58.

66. Kim, S.H., et al., *Multi-organ abnormalities and mTORC1 activation in zebrafish model of multiple acyl-CoA dehydrogenase deficiency.* PLoS Genet, 2013. **9**(6): p. e1003563.

67. Wager, K., F. Mahmood, and C. Russell, *Modelling inborn errors of metabolism in zebrafish.* J Inherit Metab Dis, 2014. **37**(4): p. 483-95.

68. Takeda, H. and A. Shimada, *The art of medaka genetics and genomics: what makes them so unique?* Annu Rev Genet, 2010. **44**: p. 217-41.

69. Indrieri, A., et al., *Mutations in COX7B cause microphthalmia with linear skin lesions, an unconventional mitochondrial disease.* Am J Hum Genet, 2012. **91**(5): p. 942-9.

70. Morita, A., et al., *Establishment and characterization of Roberts syndrome and SC phocomelia model medaka (Oryzias latipes).* Dev Growth Differ, 2012. **54**(5): p. 588-604.

71. Aller, E., et al., *Analysis of the Ush2a gene in medaka fish (Oryzias latipes).* PLoS One, 2013. **8**(9): p. e74995.

72. Indrieri, A., et al., *The impairment of HCCS leads to MLS syndrome by activating a non-canonical cell death pathway in the brain and eyes.* EMBO Mol Med, 2013. **5**(2): p. 280-93.

73. Uemura, N., et al., *Viable neuronopathic Gaucher disease model in Medaka (Oryzias latipes) displays axonal accumulation of alpha-synuclein.* PLoS Genet, 2015. **11**(4): p. e1005065.

74. Ansai S, Sakuma T, Yamamoto T, Ariga H, Uemura N, Takahashi R, Kinoshita M, *Efficient Targeted Mutagenesis in Medaka Using Custom-Designed Transcription Activator-Like Effector Nucleases.* Genetics, 2013. **193**: p. 739-749.

75. Ansai S, Inohaya K, Yoshiura Y, Schartl M, Uemura N, Takahashi R, Kinoshita M, *Design, evaluation, and screening methods for efficient targeted mutagenesis with transcription activator-like effector nucleases in medaka.* Develop. Growth Differ., 2014. **56**: p. 98-107.

76. Doyle, E.L., et al., *TAL Effector-Nucleotide Targeter (TALE-NT) 2.0: tools for TAL effector design and target prediction.* Nucleic Acids Res, 2012. **40**(Web Server issue): p. W117-22.

77. Kinoshita, M., et al., *Activity of the medaka translation elongation factor 1alpha-A promoter examined using the GFP gene as a reporter.* Dev Growth Differ, 2000. **42**(5): p. 469-78.

78. Berghmans, S., et al., *Zebrafish offer the potential for a primary screen to identify a wide variety of potential anticonvulsants.* Epilepsy Res, 2007. **75**(1): p. 18-28.

79. Levesque, S., et al., *Short-term outcome of propionic aciduria treated at presentation with N-carbamylglutamate: a retrospective review of four patients.* JIMD Rep, 2012. **2**: p. 97-102.

80. Sanchez-Alcudia, R., et al., *Feasibility of nonsense mutation readthrough as a novel therapeutical approach in propionic acidemia.* Hum Mutat, 2012. **33**(6): p. 973-80.

81. Ding, L., et al., *Quantifiable biomarkers of normal aging in the Japanese medaka fish (Oryzias latipes).* PLoS One, 2010. **5**(10): p. e13287.

82. Kurczynski, T.W., et al., *Metabolic studies of carnitine in a child with propionic acidemia.* Pediatr Res, 1989. **26**(1): p. 63-6.

83. Perez-Cerda, C., et al., *Functional analysis of PCCB mutations causing propionic acidemia based on expression studies in deficient human skin fibroblasts.* Biochim Biophys Acta, 2003. **1638**(1): p. 43-9.

84. Wu, M., I.A. Khan, and A.K. Dasmahapatra, *Valproate-induced teratogenesis in Japanese rice fish (Oryzias latipes) embryogenesis.* Comp Biochem Physiol C Toxicol Pharmacol, 2012. **155**(3): p. 528-37.

85. Shi, X., et al., *Developmental toxicity and alteration of gene expression in zebrafish embryos exposed to PFOS.* Toxicol Appl Pharmacol, 2008. **230**(1): p. 23-32.

86. He, J.H., et al., *A zebrafish phenotypic assay for assessing drug-induced hepatotoxicity.* J Pharmacol Toxicol Methods, 2013. **67**(1): p. 25-32.

87. Sperl, W., et al., *Odd-numbered long-chain fatty acids in propionic acidaemia.* Eur J Pediatr, 2000. **159**(1-2): p. 54-8.

88. Kalueff, A.V., et al., *Towards a comprehensive catalog of zebrafish behavior 1.0 and beyond.* Zebrafish, 2013. **10**(1): p. 70-86.

89. Roe, C.R. and H. Brunengraber, *Anaplerotic treatment of long-chain fat oxidation disorders with triheptanoin: Review of 15 years Experience.* Mol Genet Metab, 2015. **116**(4): p. 260-8.

90. Roe, C.R. and F. Mochel, *Anaplerotic diet therapy in inherited metabolic disease: therapeutic potential.* J Inherit Metab Dis, 2006. **29**(2-3): p. 332-40.

91. Roe, C.R., et al., *Carnitine palmitoyltransferase II deficiency: successful anaplerotic diet therapy.* Neurology, 2008. **71**(4): p. 260-4.

92. Mochel, F., et al., *Pyruvate carboxylase deficiency: clinical and biochemical response to anaplerotic diet therapy.* Mol Genet Metab, 2005. **84**(4): p. 305-12.

93. Cynober, L., *Ornithine alpha-ketoglutarate as a potent precursor of arginine and nitric oxide: a new job for an old friend.* J Nutr, 2004. **134**(10 Suppl): p. 2858S-2862S; discussion 2895S.